

PACS numbers: 42.60.By; 42.60.Jf; 42.65.Yj; 42.65.Jx; 42.70.Mp
DOI: 10.1070/QE2013v043n00ABEH015039

Influence of spatial beam inhomogeneities on the parameters of a petawatt laser system based on multi-stage parametric amplification*

S.A. Frolov, V.I. Trunov, E.V. Pestryakov, V.E. Leshchenko

Abstract. **We have developed a technique for investigating the evolution of spatial inhomogeneities in high-power laser systems based on multi-stage parametric amplification. A linearised model of the inhomogeneity development is first devised for parametric amplification with the small-scale self-focusing taken into account. It is shown that the application of this model gives the results consistent (with high accuracy and in a wide range of inhomogeneity parameters) with the calculation without approximations. Using the linearised model, we have analysed the development of spatial inhomogeneities in a petawatt laser system based on multi-stage parametric amplification, developed at the Institute of Laser Physics, Siberian Branch of the Russian Academy of Sciences (ILP SB RAS).**

Keywords: *petawatt laser system, spatial heterogeneity, small-scale self-focusing, parametric amplification, femtosecond pulses.*

1. Introduction

The method of optical parametric amplification of few-cycle pulses opens the way for the development of a new type of laser source with extremely short pulse duration and intensity exceeding 10^{23} W cm^{-2} [1–3]. Laser radiation in such systems is strongly influenced by nonlinear effects associated with amplification of spatial intensity inhomogeneities in the beam cross section, which may lead to significant deterioration of the amplified beam profile, or even to a breakdown of optical elements.

The main mechanism of amplification of spatial inhomogeneities in high-power laser systems is a small-scale self-focusing caused by the third-order nonlinearity [4–6]. This issue has been comprehensively investigated for the case of laser amplification, but the development of small-scale self-focusing for parametric amplification still remains unexplored. Unlike laser amplification, parametric amplification is an instantaneous phase-sensitive process (at characteristic times of less than 1 fs), i.e., depends on the instantaneous values of the field at a given point in space and time. As a result, the behaviour of small-scale self-focusing can change markedly compared to the case of laser amplification, in particular due to such effects as reverse energy transfer from the amplified beam to the pump beam. For example, Ginzburg et al. [7] considered the influence of small-scale self-focusing on second harmonic generation in an intense laser field. Using the Bespalov–Talanov theory [4], Ginzburg et al. developed a linearised model, which allowed the maximally admissible level of spatial inhomogeneities to be determined for the fundamental radiation beam. In particular, the results of paper [7] show a significant difference in the gain spectrum of small-scale inhomogeneities during the radiation propagation in a cubic-nonlinearity medium and second harmonic generation in such a medium.

In this paper, in order to study the development of small-scale self-focusing during the parametric amplification, we have developed and analysed for the first time the linearised system of equations describing the noncollinear parametric interaction. We have studied the applicability of the developed model to compare it, in particular, with the results obtained by solving the complete (non-linearised) system of equations. Based on the model we have proposed a method for analysing the inhomogeneity gain, used in the petawatt laser system based on multi-stage parametric amplification in BBO crystal and LBO, developed at the ILP SB RAS [2].

2. Simulation of inhomogeneity development

2.1. Models describing the development of inhomogeneities

The development of inhomogeneities can be simulated in two ways [8]. The first approach involves direct modelling of inhomogeneities with different initial parameters – an amplitude and a phase. In this paper, the simulation was carried out by solving a system of truncated parametric amplification equations, extended to take into account diffraction, birefringence, self- and cross-phase modulation [8, 9]:

$$\frac{\partial A_\mathrm{s}}{\partial z} = \hat{L}_\mathrm{s} A_\mathrm{s} + \mathrm{i}\sigma_s A_\mathrm{i}^* A_\mathrm{p} \mathrm{e}^{\Delta k z} + \mathrm{i}\frac{\omega_\mathrm{s}}{c}\left(\gamma_{\mathrm{ss}}\left|A_\mathrm{s}\right|^2 + \gamma_{\mathrm{si}}\left|A_\mathrm{i}\right|^2 + \gamma_{\mathrm{sp}}\left|A_\mathrm{p}\right|^2\right)A_\mathrm{s},$$

$$\frac{\partial A_\mathrm{i}}{\partial z} = \hat{L}_\mathrm{i} A_\mathrm{i} + \mathrm{i}\sigma_\mathrm{i} A_\mathrm{s}^* A_\mathrm{p} \mathrm{e}^{\Delta k z} + \mathrm{i}\frac{\omega_\mathrm{i}}{c}\left(\gamma_{\mathrm{ii}}\left|A_\mathrm{i}\right|^2 + \gamma_{\mathrm{is}}\left|A_\mathrm{s}\right|^2 + \gamma_{\mathrm{ip}}\left|A_\mathrm{p}\right|^2\right)A_\mathrm{i}, \quad (1)$$

* Presented at the Laser Optics Conference, St. Petersburg, Russia, June 2012.

S.A. Frolov, V.I. Trunov, E.V. Pestryakov, V.E. Leshchenko Institute of Laser Physics, Siberian Branch, Russian Academy of Sciences, prosp. Akad. Lavrent'eva 13/3, 630090 Novosibirsk, Russia; e-mail: pefvic@laser.nsc.ru

Received 24 October 2012; revision received 12 February 2013
Kvantovaya Elektronika **43** (5) 481–488 (2013)
Translated by I.A. Ulitkin

$$\frac{\partial A_{\rm p}}{\partial z} = \hat{L}_{\rm p}A_{\rm p} + {\rm i}\sigma_{\rm p}A_i A_{\rm s}{\rm e}^{-\Delta kz} + {\rm i}\frac{\omega_{\rm p}}{c}\left(\gamma_{\rm pp}\left|A_{\rm p}\right|^2 + \gamma_{\rm pi}\left|A_{\rm i}\right|^2 + \gamma_{\rm ps}\left|A_{\rm s}\right|^2\right)A_{\rm p},$$

$$\hat{L}_m A_m = {\rm i}F_-\left[\left(\frac{k_m}{\cos(k_\perp/k_m)} - k_{m0} - \frac{\omega_m - \omega_{m0}}{v_{\rm g}}\right)F_+[A_m]\right],$$

where

$$k_m = n_m(\omega_m, \theta + k_x/k_m)\frac{\omega_m}{c};$$

$$k_{m0} = n_m(\omega_{m0}, \theta)\frac{\omega_{m0}}{c}, k_\perp = \sqrt{k_x^2 + k_y^2};$$

$$\Delta k = k_{{\rm p}0z} - k_{{\rm s}0z} - k_{{\rm i}0z};$$

$\varepsilon_m = A_m\exp(-{\rm i}\omega_m t + {\rm i}k_{m0z}z)$ is the electric field strength of the wave m; A_m is the electric field envelope (hereafter m = s, i, p is a signal wave, idler wave and pump wave, respectively); σ_m is the second-order nonlinearity coefficient; γ_{mn} is the nonlinear refractive index, which characterises the phase modulation of the wave m by the wave n (n = s, i, p); ω_m is the frequency of the wave m; ω_{m0} is the carrier frequency of the wave m; k_m is the wave vector; v_g is the group velocity of the pump; $k_{m0z} = k_{m0}\cos\alpha_m$; α_m is the angle of the wave vector of the wave m with the axis z; n_m is the refractive index of the medium; θ is the angle with the optical axis of the crystal; F_+, F_- are the operators of the direct and inverse Fourier transform, respectively; and Δk is the wave detuning.

By expanding the refractive index in the expression for the wave vector and the cosine in the denominator of the first term of the operator $\hat{L}_m$ by k_x and k_y, this system is reduced to the well-known truncated equations with drift and diffraction operators. Also, system (1) can be derived using the approach described in [10], by maintaining the angular dependence of the wave vector and by substituting $E = A_{\rm s}\times\exp(-{\rm i}\omega_{\rm s}t + {\rm i}k_{{\rm s}z}z) + A_{\rm i}\exp(-{\rm i}\omega_{\rm i}t + {\rm i}k_{{\rm i}z}z) + A_{\rm p}\exp(-{\rm i}\omega_{\rm p}t + {\rm i}k_{{\rm p}z}z)$. Thus, the system of equations can simulate all the effects that make a significant contribution to the evolution of inhomogeneities. This approach to modelling the inhomogeneities suggests a significant number of time-consuming calculations and their analysis.

Another approach, first proposed for modelling the development of inhomogeneities during the parametric amplification, makes it possible to simultaneously carry out the calculations for a wide range of parameters of spatial perturbations. The main idea is to simulate inhomogeneities as a small correction to the fundamental field [4, 7]. This assumption allows us to derive a linear system of equations for the perturbation field. Since such a system of equations is cumbersome, we present below only one of the equations (the complete system includes six equations)

$$\frac{{\rm d}A_{{\rm s},1}}{{\rm d}z} = \frac{-{\rm i}}{\cos(\alpha + \alpha_{12})\cos\alpha_{11}}\left\{\sigma_{\rm s}\left(E_{{\rm p},0}E^*_{{\rm i},2} + E_{{\rm p},1}E^*_{{\rm i},0}\right) + \frac{\omega_{\rm s}}{c}\left[\gamma_{\rm ss}\left(2\left|E_{{\rm s},0}\right|^2E_{{\rm s},1} + E^2_{{\rm s},0}E^*_{{\rm s},2}\right) + \gamma_{\rm si}\left(\left|E_{{\rm i},0}\right|^2E_{{\rm s},1} + \left(E_{{\rm i},0}E^*_{{\rm i},2} + E_{{\rm i},1}E^*_{{\rm i},0}\right)E_{\rm s}\right) + \gamma_{\rm sp}\left(\left|E_{{\rm p},0}\right|^2E_{{\rm s},1} + \left(E_{{\rm p},0}E^*_{{\rm p},2} + E_{{\rm p},1}E^*_{\rm p}\right)E_{{\rm s},0}\right)\right]\right\}\exp({\rm i}k_{{\rm s},1z}z), \quad (2)$$

where $k_{{\rm s},0z} = k_{\rm s}\cos\alpha$; $k_{{\rm s},jz} = k_{\rm s}\cos\alpha_{j1}\cos(\alpha + \alpha_{j2})$, j = 1, 2; $E_{m,j} = A_{m,j}\exp(-{\rm i}k_{m,jz}z)$, j = 0, 1, 2 (the zero subscript corresponds to the field of the fundamental wave, and 1 and 2 – to angular components of the inhomogeneity of a single wave; the sum of the projections of the wave vector of these components at the front face of the crystal is equal to zero); α is the angle between the amplified wave and the pump wave in a noncollinear scheme; the remaining arguments in the trigonometric functions are small angles of the inhomogeneity components with the fundamental wave, the first subscript corresponding to the direction of the inhomogeneity wave, and the second – to the plane: 1 – critical to synchronism, 2 – uncritical.

As far as we know, such a linearised model that takes into account the parametric amplification and self-focusing is proposed for the first time. It allows one to assess the angular distribution of the complex gain of the perturbation field, which makes it possible to calculate the evolution of arbitrary spatial inhomogeneities. The obvious disadvantage of the model is the inability to account for a number of effects, such as changes in the profile of the perturbations due to diffraction, saturation of parametric amplification, etc. Thus, it is important to know the range of applicability of the model. The next part of the work is devoted to the study of the range of applicability of the model for a number of specific cases.

2.2. Effective cubic susceptibility for LBO and BBO crystals

To determine the effect of small-scale self-focusing on the evolution of inhomogeneities, it is important to use the most accurate value of γ_{mn} in equations (1) and (2). Below we present the experimental data on the cubic nonlinear susceptibility tensor and interpret them in order to obtain the values of these coefficients for the BBO and LBO crystal used in our petawatt system. The expressions for the effective cubic susceptibility in self- and cross-phase modulation can be easily derived from the crystal symmetry and Kleinman's rules [11, 12]. The expressions obtained for BBO and LBO crystals (only in the XY plane) are presented in Table 1.

The tensor components (χ_{im}) for the BBO crystal were taken from [13]: χ_{11} = 503 pm^2 V^{-2}, χ_{10} = –24 pm^2 V^{-2}, χ_{16} = 146 pm^2 V^{-2}, and χ_{33} = –104 pm^2 V^{-2}. Despite the anomalous value of χ_{33}, this component does not have a significant impact on the effective cubic nonlinearity coefficient for the phase-matching angles in question. For the LBO crystal the data are scarce. The measured values of n_2 [14] gave χ_{11} = 236 pm^2 V^{-2} and χ_{22}=173 pm^2 V^{-2}. The component χ_{33} = 244 pm^2 V^{-2} was obtained from the formula for the effective cubic susceptibility $\chi^{(3)}_{\rm eff}$ [15] from the components χ_{11} and χ_{22}:

$$\frac{\chi^{(3)}_{\rm eff\,1}}{\chi^{(3)}_{\rm eff\,2}} = \frac{(n^2_{01} - 1)}{(n^2_{02} - 1)}\frac{\partial n^2_{01}}{\partial\lambda}\left(\frac{\partial n^2_{02}}{\partial\lambda}\right)^{-1}, \quad (3)$$

where $\chi^{(3)}_{{\rm eff}\,i}$ is the effective cubic susceptibility; n_{0i} is the refractive index for configuration i. We have chosen this approach because the formula (3) has yielded good results when calculating the coefficient χ_{11} from the coefficient χ_{22} and back for the LBO crystal (with accuracy up to 5%), and for the KTP crystal having the same symmetry mm2 [16] (with accuracy up to 10%). The components χ_{16} = 80 pm^2 V^{-2}, χ_{18}=68 pm^2 V^{-2} and χ_{24} = 70 pm^2 V^{-2} for the LBO crystal were evaluated in the approximation of an isotropic medium as $\chi_{16} = (\chi_{11} + \chi_{33})/6$,

Table 1. Expressions for effective cubic susceptibilities in case of self- and cross-phase modulation in BBO and LBO crystals.

Crystal	Polarisation*	Expression
BBO (symmetry 3m)	o–o	$\chi^{(3)}_{\text{eff}} = \chi_{11}$
	e–e	$\chi^{(3)}_{\text{eff}} = \chi_{11}\cos^4\theta + \frac{3}{2}\chi_{16}\sin^2 2\theta - 2\chi_{10}\cos^2\theta \sin 2\theta \sin 3\varphi + \chi_{33}\sin^4\theta$
	o–e, e–o	$\chi^{(3)}_{\text{eff}} = \frac{1}{3}\chi_{11}\cos^2\theta + \chi_{16}\sin^2\theta + \chi_{10}\sin 2\theta \sin 3\varphi$
LBO (symmetry mm2), XY plane	o–o	$\chi^{(3)}_{\text{eff}} = \chi_{33}$
	e–e	$\chi^{(3)}_{\text{eff}} = \chi_{11}\sin^4\varphi + \frac{3}{2}\chi_{18}\sin^2 2\varphi + \chi_{22}\cos^4\varphi$
	o–e, e–o	$\chi^{(3)}_{\text{eff}} = \chi_{16}\sin^2\varphi + \chi_{24}\cos^2\varphi$

* The first symbol indicates the polarisation of the wave, which experiences modulation, the second – the polarisation of the modulating wave, i.e., for example, o – e means the ooe → e interaction.

Table 2. The values of the coefficients γ_{mn}.

Crystal	$\gamma_{ss}, \gamma_{ii}/10^{-16}$ cm^2 W^{-1}	$\gamma_{si}, \gamma_{is}/10^{-16}$ cm^2 W^{-1}	$\gamma_{sp}, \gamma_{ps}/10^{-16}$ cm^2 W^{-1}	$\gamma_{ip}, \gamma_{pi}/10^{-16}$ cm^2 W^{-1}	$\gamma_{pp}/10^{-16}$ cm^2 W^{-1}
BBO ($\theta = 23.7°$, $\varphi = 90°$)	5.16	10.32	3.72	3.72	4.26
LBO (XY plane, $\varphi = 11.8°$)	2.68	5.36	1.55	1.55	1.94

$\chi_{18} = (\chi_{11} + \chi_{22})/6$ and $\chi_{24} = (\chi_{22} + \chi_{33})/6$. Thus, using the above values of the components of the cubic nonlinearity tensors we have calculated effective values of the cubic nonlinearity coefficient γ_{mn} (Table 2).

3. Analysis of the models

3.1. Applicability of the linearised model

As noted above, the linearised equations of parametric amplification with the nonlinear self- and cross-phase modulation taken into account have limited ranges of applicability. Below we consider the ranges for the cases of nonlinear propagation and parametric amplification. Since the boundaries of these ranges depend on the parameters of a specific problem, we have investigated their most characteristic range. To determine the deviation of the calculation results in the linearised approximation from the results of model (1), we have performed a comparison under the following assumptions: the spatial shape of the perturbation is Gaussian, and the spatial profile of the fundamental beams is super-Gaussian (eighth order). The latter allows us to reconstruct the conditions of the fundamental radiation profile, given in model (2). Then, we calculate the complex angular gain of the field in the complete model:

$$g_{\text{direct}} = \frac{F_+(A_{iL} - A_{0L})}{F_+(A_{i0} - A_{00})}, \tag{4}$$

where the first subscript i(0) indicates the presence (absence) of inhomogeneities in the beam, and the second subscript $L(0)$ corresponds to the output (input) crystal face. The angular gain of the field in the linearised model has the form

$$g_{\text{lin}} = \frac{A_{\text{lin}L}}{A_{\text{lin}0}}, \tag{5}$$

where $A_{\text{lin}L}$ is the amplified perturbation field in the linearised model at the output of the medium, and $A_{\text{lin}0}$ is the initial wave field, which causes perturbation. Knowing both gains in the linearised model and the direct calculation, we estimate the error Δ as follows:

$$\Delta = \frac{\int\int |\, g_{\text{direct}}(\alpha_1,\alpha_2) - g_{\text{lin}}(\alpha_1,\alpha_2)\,|^2 \mathrm{d}\alpha_1 \mathrm{d}\alpha_2}{\int\int |\, g_{\text{direct}}(\alpha_1,\alpha_2)\,|^2 \mathrm{d}\alpha_1 \mathrm{d}\alpha_2}, \tag{6}$$

where the integration is performed over the angles, in which the gain with respect to the intensity exceeds e^{-2} of the peak value. It is important to note that the gains include phase characteristics of amplified perturbations, which, as will be shown below, are important for the correct reconstruction of the amplified perturbation profile.

First, we consider the case of nonlinear propagation of the pump wave only in an isotropic medium, i.e., from nonlinear effects only self-phase modulation will be taken into account. This process is characterised by a B-integral:

$$B = \int_0^L k_0 \gamma I_{\text{peak}}(z)\,\mathrm{d}z, \tag{7}$$

where k_0 is the wave vector in a vacuum; γ is a nonlinear refractive index; I_{peak} is the peak intensity; and L is the length of the medium. The simulation was performed for a short (0.1 cm) and long (10 cm) TF-8 glass block ($\gamma = 9.69\times10^{-16}$ cm^2 W^{-1}) for the B integral ranging from 1 to 4 rad, the emission wavelength of 532 nm and the inhomogeneity radius of 50 μm. These parameters correspond to the most effective inhomogeneity component gain with the angle 10–20 and 1–2 mrad between the wave vectors of the perturbation and fundamental wave for L = 0.1 and 10 cm, respectively. This choice allows one to conduct a study both in the case of weak and strong contribution of diffraction. Figure 1 shows the dependence of the error Δ on the ratio of the peak intensity of the inhomogeneity, I_{ihm}, to the peak intensity of the fundamental beam, I_0. Good agreement of the results in a wide range of perturbation intensities, especially for small values of the B-integral, is caused by the smallness of the inhomogeneity gain due to self-focusing.

Next, we consider the case of parametric amplification of 800-nm radiation under pumping at 532 nm with an intensity of 10 GW cm^{-2} in the BBO crystal with the noncollinearity angle 2.3° (d_{eff} for these parameters is 2.1 pm V^{-1}). The inten-

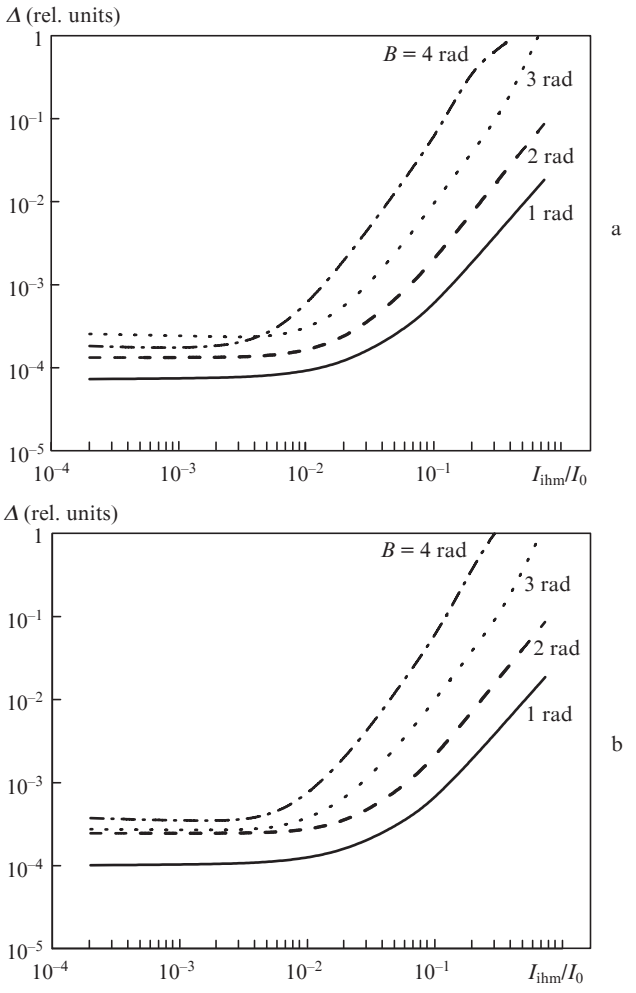

Figure 1. Comparison of the calculation results obtained by the linearised model with direct calculations for (a) short (0.1 cm) and (b) long (10 cm) TF-8 glass block.

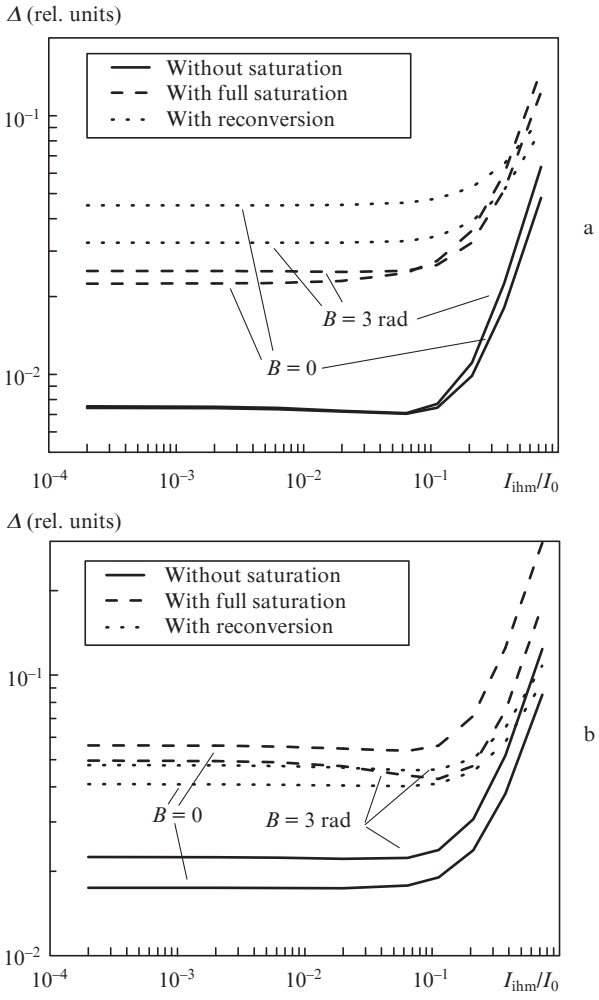

Figure 2. Comparison of the models for the case of parametric amplification for the gains $G =$ (a) 100 and (b) 10000.

sity of the amplified radiation and the crystal length were chosen so as to achieve the desired gain and saturation. We considered the gains 10^2 and 10^4 in the absence of gain saturation in the case of saturation to the maximum gain level (full saturation) and up to the 70% level underreconversion. To study the effect of large B-integrals, we considered the cases with an increased cubic nonlinearity coefficient γ. When performing calculations, the inhomogeneity was initially present in the pump, and the comparison was made for the inhomogeneity resulting in an amplified wave.

The results of the comparison are presented in Fig. 2. The data obtained within the framework of the linearised model sufficiently well coincide with direct calculation. Basically, the error is introduced by smoothing the inhomogeneities due to diffraction. It is also important to note that the linearised model properly accounts for birefringence in the crystal because its effect on the evolution of small inhomogeneities (100–500 μm) is significant. Phase effects will be discussed in more detail in Section 4.

3.2. Interpretation of the results of the model

As noted above, the result of the calculation of the evolution of inhomogeneities under parametric amplification in the linearised model is the angular gain spectrum of their field. Since the gain spectrum comprises a phase change, it plays an important role in determining the resulting total field of the fundamental wave and its amplified inhomogeneity. For example, in the case of beam propagation in a medium with cubic nonlinearity the phase accumulated by an unperturbed beam is different from the phase of the perturbed beam due to the difference in the intensities. Obviously, a weak field, as a solution to equation (2), must include the phase change. For example, in a direction at a small angle to the propagation axis of the fundamental wave, the initial-phase-averaged gain of the small addition to the fundamental field intensity due to the self-phase modulation will be approximately equal to $2B^2 + 1$ [7]. Considering the evolution of a sufficiently large perturbation, it is easy to understand that its intensity remains the same, because it is not subjected to self-focusing, and only the phase changes. Nevertheless, using the intensity gain [7], the intensity of the beam propagating in a medium with a cubic nonlinearity evolves when it is impossible in principle. However, using the calculated complex gain for obtaining the resulting total field, it can be shown that the field intensity remains constant with high accuracy, and the estimated accumulated phase closely matches the exact solution, this difference being due to the approximations used. It follows that for a correct analysis of the real growth of perturbations it is crucial to reconstruct the total field of the perturbation and the

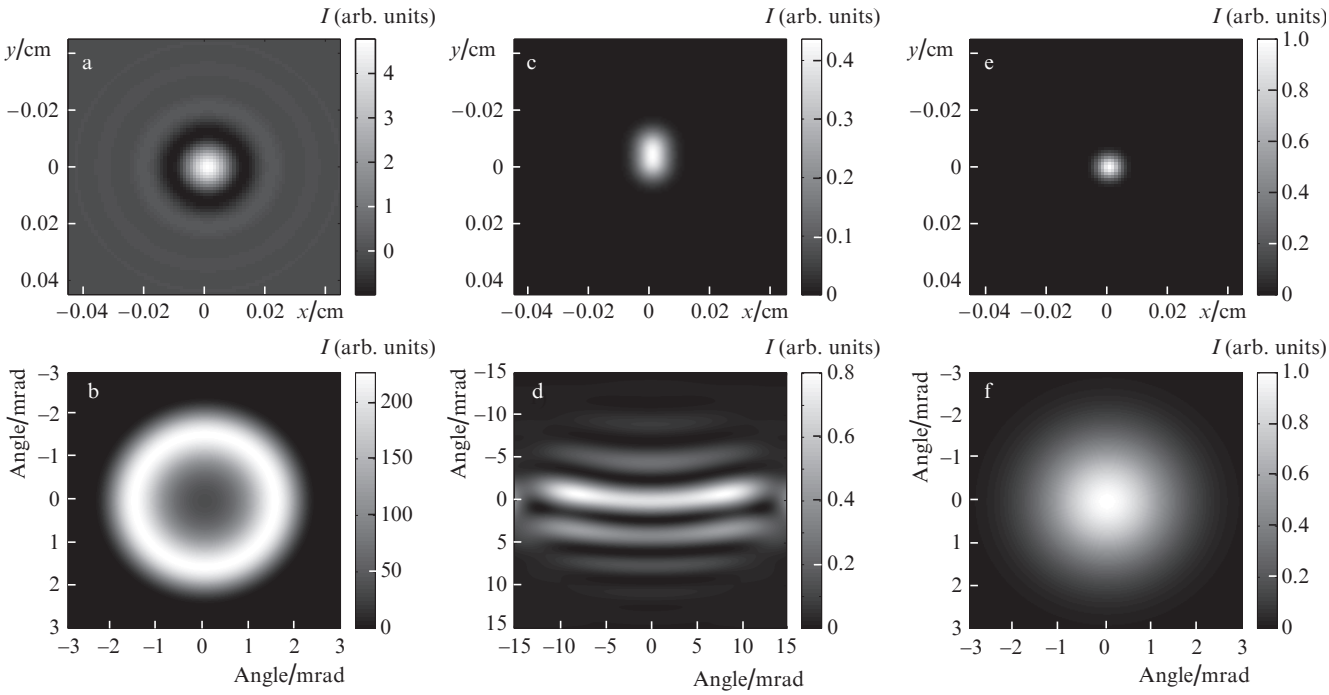

Figure 3. (a, c) Typical spatial profiles of the amplified inhomogeneity and (b, d) angular gain spectra obtained in the simulations of the inhomogeneity gain in the case of (a, b) nonlinear propagation ($B = 3$ rad, $L = 10$ cm) and (c, d) parametric amplification ($G = 100$) upon saturation to the maximum gain. For comparison are presented (e) the initial spatial profile and (f) the angular spectrum of the inhomogeneity corresponding to the divergence of 2 mrad.

fundamental wave on the basis of the complex gain. As one of the most important quantitative characteristics of the growth of inhomogeneities is their peak intensity, the evolution of inhomogeneities will be analysed by using the peak intensity gain, taking into account the phase characteristics of the inhomogeneities, which is given by the expression for a given spatial perturbation profile A_{inh}:

$$g_{\text{peak}} = \sup\left[\frac{\left|F_{-}\{g_{\text{lin}}F_{+}\{A_{\text{inh}}\}\} + A_{sL}\right|^2 - \left|A_{sL}\right|^2}{\left|A_{sL}\right|^2}\right] \times \frac{\max\left|A_{\text{p0}}\right|^2}{\max\left|A_{\text{inh}}\right|^2}, \quad (8)$$

where sup means both a minimum and a maximum value of the inhomogeneity profile. It follows from formula (8), for example, that at the initial perturbation of the pump with a 10% amplitude from its peak intensity and at a gain 2 at the output, the amplified wave will have a peak that is 20% of its peak intensity, and at a gain –2 – a dip of 20%.

Figures 3a and b show the angular inhomogeneity gains with respect to intensity and the calculated resulting spatial profile of the inhomogeneity in the case of a Gaussian initial distribution with the divergence of 2 mrad during the propagation of 532-nm radiation in a 10-cm-long TF-8 glass block at $B = 3$ rad. The initial profiles are shown in Figs 3e and f. It is particularly noteworthy that a significant gain at zero angles does not lead to amplification of large size inhomogeneities, but only changes their nonlinear phase incursion, which is observed in the calculation in the complete model.

Unlike cubic nonlinearity, parametric amplification does not contribute significantly to the phase of the amplified beam. Such a contribution is possible, for example, at small-size inhomogeneities due to birefringence [17], which is observed in Figs 3c and d in the case of parametric amplification with $G = 100$ and saturation to the maximum gain. It also follows from Figs 3c and d that the discrepancy between the peak intensity gain and the maximum of the angular intensity gain spectrum is caused by the 'stretching' of the spatial profile due to birefringence. In general, the data presented show that the use of the intensity gain to study the inhomogeneity gives incorrect results. Thus, the analysis of inhomogeneities requires the calculation of their resulting profile with the phase taken into account, especially in the case of a significant contribution of cubic nonlinearity. In Section 4 we consider the technique for estimating the growth of inhomogeneities by the peak intensity gain.

4. Analysis of inhomogeneities in the petawatt laser system

Currently, the ILP SB RAS is developing a scheme of a petawatt laser system based on multi-stage parametric amplification with picosecond pumping (Fig. 4). The system is characterised by high pump intensity due to picosecond pump pulse duration, which makes it possible to use it with high efficiency. The parameters of the system are selected with the help of numerical simulations [2]. Thus, in the first stage use is made of the BBO crystal, because it has a high nonlinearity and a broad gain spectrum. The use of LBO crystals for subsequent stages is a compromise between high nonlinearity with a broad gain spectrum and a large available aperture. Simulations have shown that for such a system to be realised, the LBO crystal aperture should be 100–120 mm. The pump energy at each stage is selected such that it has a maximum intensity from the standpoint of resistance to optical breakdown; this allows the conversion efficiency of about 30%. In this case, the B-integral of the entire system is equal to

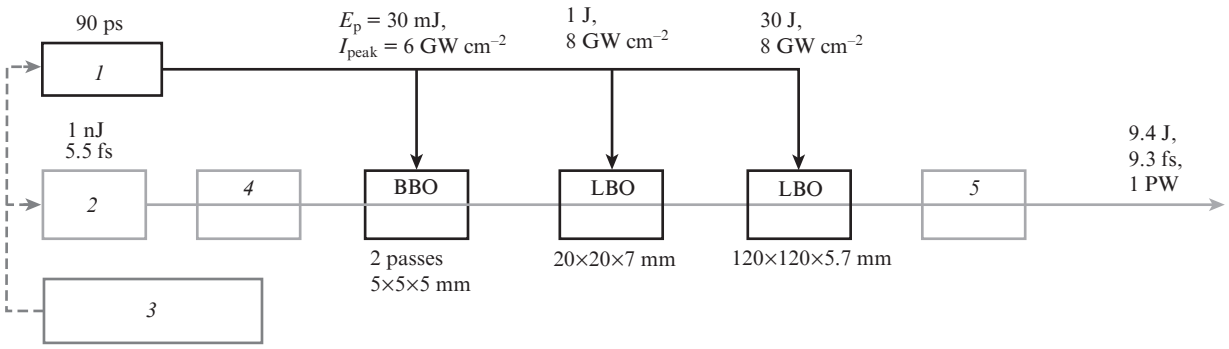

Figure 4. Scheme of a petawatt laser system: (*1*) picosecond pump laser with a pulse duration of 90 ps; (*2*) femtosecond laser; (*3*) frequency standard; (*4*) stretcher; (*5*) compressor; I_{peak} is the peak intensity of the pump; E_p is the pump energy.

0.45 rad, and the *B*-integral in a single stage does not exceed 0.2 rad.

In the case of our petawatt system, the inhomogeneities under parametric amplification can be divided into large- and small-scale ones. The former are amplified mainly due to parametric amplification, the latter – due to small-scale self-focusing, and the boundary between them is roughly equivalent to the angular width of the phase matching of nonlinear crystals. The divergence of the small-scale inhomogeneities, corresponding to characteristic parameters of the laser systems based on parametric amplification stages with picosecond pumping (the length of the crystals is a few millimetres, the radiation intensity is ~10 GW cm^{-2}), as follows from the results of the calculations, lies in the range of 5–15 mrad, i.e., typically lies outside the angular phase-matching width of nonlinear crystals, and the parametric amplification occurs in a narrow band of the angular spectrum. The exception is a crystal with a large angular phase matching width, such as LBO.

Also, in the absence of spatial filtration when the beam size between the stages changes, small-scale inhomogeneities can undergo transition into large-scale ones and will be amplified by the parametric process; as shown below, they may be suppressed. The large-scale inhomogeneity gain is determined by the degree of gain saturation. Thus, in the case of gain without saturation they are characterised by a significant positive gain, whereas in the case of reconversion, the gain will be negative; when the maximum gain is saturated up to a certain level, it may be equal to zero. In this case, large-scale inhomogeneities, unlike small-scale ones, cannot be suppressed by spatial filtering; therefore, it is especially important to perform an analysis of the inhomogeneity gain in all the stages of the laser system in order to reduce the net gain. Next, using the linearised model we have analysed the development of spatial perturbations in the petawatt system for its three stages. Within the framework of the analysis of the inhomogeneity evolution we consider the dependence of the gain on their size, taking into account the parametric amplification and nonlinear phase modulation. We assume that initial perturbation is present in the pump, and its evolution is considered in the amplified wave. The results of calculations for the different sets of the effects taken into account are shown in Fig. 5.

Let us consider first the effect of the nonlinear phase modulation without parametric amplification (Figs 5a–c). With these parameters of our system, small-scale self-focusing leads to the most significant amplification of small inhomogeneities, in this case, with the divergence of 9 mrad for the first stage and 8 mrad for the second and third stages. As might be expected, at large *B*-integrals for which calculations were carried out, the inhomogeneities will be significantly amplified; however, in the first stage the gain is very small due to birefringence and noncollinearity in the stage with the BBO crystal, which introduce 'walk-off' of the inhomogeneity in the pump relative to the signal wave and do not produce a significant intensity perturbation in the amplified wave. This is confirmed by calculations: in the absence of birefringence and noncollinearity, the gain is equal to 5, and in the presence of birefringence – to 1.1. For this reason, due to lower birefringence in LBO crystals in the second stage, a larger peak gain is observed. However, in the third stage due to resizing and the absence of the spatial filtration, the amplified peak is shifted to 1–2 mrad; in this case, as a result of small-scale self-focusing a new peak is formed, centred at 6–8 mrad.

As was mentioned above, in parametric amplification the characteristic determining the inhomogeneity gain is the degree of saturation which is demonstrated by our results (Figs 5d–f). The first stage ensures the reconversion and, therefore, has a considerable negative gain. The other stages of the petawatt system are configured to saturate to a level of the maximum gain; therefore, large-scale spatial perturbations are considerably suppressed. At a high nonlinear phase modulation, the dependence in the region of 5–20 mrad, exceeding the angular phase-matching width of parametric amplification, becomes mainly the same as in the absence of parametric amplification (Figs 5a–c). The exception is the last stage where the gain at larger angles is significant and makes a greater contribution to the net gain due to the saturation of the parametric amplification. The greatest change occurs in the transition region of 1–5 – mrad, where the contribution of parametric amplification is already significant. One can see that the inhomogeneity in the form of peaks from the previous stage is suppressed by gain saturation, and inhomogeneities in the form of dips are amplified.

Thus, the numerical simulations show that the growth of large-scale inhomogeneities in the developed petawatt system is limited by the operation of the stages in the saturation regime, while small-scale inhomogeneities do not develop because of the smallness of the *B*-integral. It is also shown that in the case of parametric amplification with a large *B*-integral, quantitative parameters change compared with the propagation without amplification. Changes mainly occur

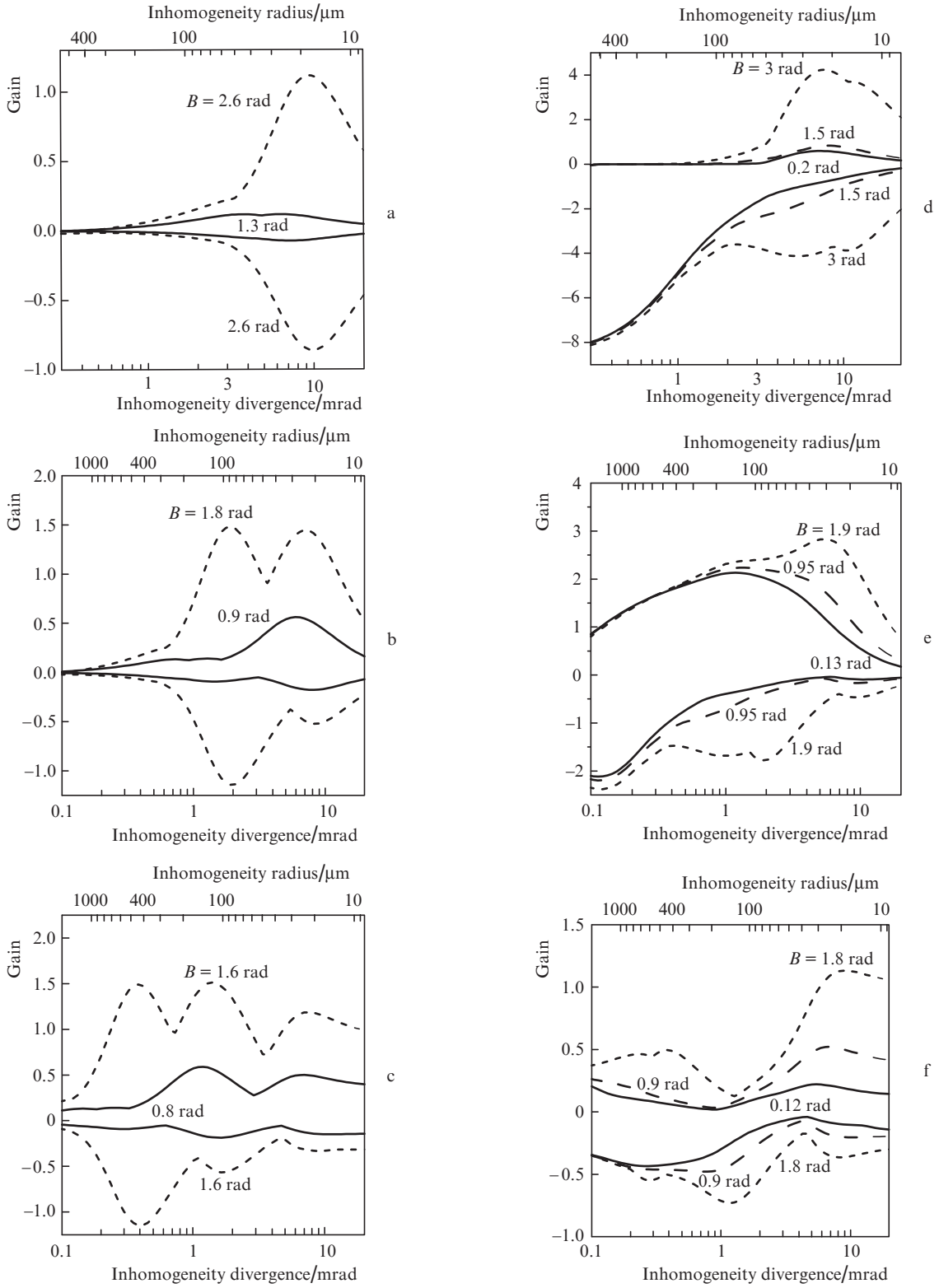

Figure 5. Peak intensity inhomogeneity gain as a function of the inhomogeneity size (maximum and minimum values of the profile are presented): (a, b, c) the impact of nonlinear phase modulation and (d, e, f) parametric amplification at the (a, d) first, (b, e) second and (c, f) third stages.

in the transition region (1–5 mrad), but also take place in the region, typical of small-scale inhomogeneities (5–20 mrad). It is also important to note that the parametric amplification can significantly suppress the amplified inhomogeneities from the previous stage due to telescoping of the beams between the stages when the size of the beams changes.

5. Conclusions

A linearised model is proposed for the first time to calculate the evolution of perturbations in high-power laser systems based on parametric amplification. The use of such a model has some significant advantages over direct simulation,

because the angular gain spectrum is obtained, which allows one to calculate the increase in the inhomogeneity of any size and profile.

The linearised model can be used in a wide range of the perturbations parameters for nonlinear propagation and for parametric amplification, including at large B-integrals. The study of phase characteristics of the angular inhomogeneity gain spectrum in the problems of nonlinear propagation and parametric amplification shows that the intensity gain in inhomogeneities does not reflect the real growth of perturbations. Even at large intensity gains ($\sim 10^2$), the increase in the peak intensity, in calculations employing the complex gain, may be reduced by two orders of magnitude. For this reason, we have developed a method for analysing the peak inhomogeneity intensity gain, which allows us to estimate their real change.

Using the technique developed, we have analysed the evolution of the inhomogeneities in the developed scheme of the petawatt laser system based on multi-stage parametric amplification. The calculations for the nonlinear propagation and parametric amplification with both low and high cubic nonlinearity have made it possible to determine the influence of each of the effects of the inhomogeneity gain. It is established that in the case of small-scale inhomogeneities (divergence of 5–20 mrad), in the amplified wave of greatest influence is birefringence, while the effect of parametric amplification is quite weak. On the other hand, in the transition region (1–5 mrad), the inhomogeneity gain varies significantly (due to suppression of inhomogeneities from the previous stage by parametric amplification).

Thus, the linearised model and method of analysis allow us to study the development of inhomogeneities of any size and shape in high-power laser systems based on multi-stage parametric amplification. This opens up the possibility of developing the methods of small-scale self-focusing suppression, taking into account the parametric amplification, which will finally improve the parameters of high-power laser systems.

Acknowledgements. This work was partially supported by the programme 'Extreme Light Fields and Their Applications' of the Presidium of the Russian Academy of Sciences, by the Russian Ministry of Education and Science of the Russian Federation (Agreement 8387), and by the Russian Foundation for Basic Research (Grant No. 12-02-31856_mol-a).

The authors express their gratitude to S.N. Bagayev for the support of this work.

References

1. Bagayev S.N., Pestryakov E.V., Trunov V.I. *Opt. Atmos. Okean.*, **23**, 845 (2010).
2. Pestryakov E.V., Petrov V.V., Trunov V.I., Frolov S.A., Kirpichnikov A.V., Kokh A.E., Bagaev S.N. *Proc. SPIE Int. Soc. Opt. Eng.*, **7994**, 799425 (2011).
3. Major Z., Trushin S.A., Ahmad I., et.al. *Rev. Laser Eng.*, **37**, 431 (2009).
4. Bespalov V.I., Talanov V.I. *Pis'ma Zh. Eksp. Teor. Fiz.*, **3**, 471 (1966).
5. Rozanov N.N., Smirnov V.A. *Kvantovaya Elektron.*, **7**, 410 (1980) [*Sov. J. Quantum Electron.*, **10**, 232 (1980)].
6. Garanin S.G., Epatko I.V., L'vov L.V., Serov R.V., Sukharev S.A. *Kvantovaya Elektron.*, **37**, 1159 (2007) [*Quantum Electron.*, **37**, 1159 (2007)].
7. Ginzburg V.N., Lozhkarev V.V., Mironov S.Yu., Potemkin A.K., Khazanov E.A. *Kvantovaya Elektron.*, **40**, 503 (2010) [*Quantum Electron.*, **40**, 503 (2010)].
8. Frolov S.A., Trunov V.I., Pestryakov E.V., Kirpichnikov A.V., Petrov V.V. *Opt. Atmos. Okean.*, **25**, 278 (2012).
9. Yates M.A., Tsangaris C.L., Kinsler P., New G.H.C. *Opt. Commun.*, **257**, 164 (2006).
10. Kinsler P. *Phys. Rev. A*, **81**, 013819 (2010).
11. Sirotin Yu.I., Shaskol'skaya M.P. *Osnovy kristallofiziki* (Fundamentals of Crystal Physics) (Moscow: Nauka, 1979).
12. Midwinter J.E., Warner J.Br. *J. Appl. Phys.*, **16**, 1665 (1965).
13. Bache M., Guo H., Zhou B., Zeng X. *Opt. Mater.Express* (to be published).
14. Li H.P., Kam C.H., Lam Y.L., Ji W. *Opt. Mater.*, **15**, 237 (2001).
15. Ganeev R.A., Kulagin I.A., Ryasnyansky A.I., Tugushev R.I., Usmanov T. *Opt. Commun.*, **229**, 403 (2003).
16. DeSalvo R., Sheik-Bahae M., Said A.A., Hagan D.J., Van Stryland E.W. *Opt. Lett.*, **18**, 194 (1993).
17. Wei X., Qian L., Yuan P., Zhu H., Fan D. *Opt. Express*, **16**, 8904 (2008).